

Dynamical effects of spin-dependent interactions in low- and intermediate-energy heavy-ion reactions

Jun Xu,^{1,2,*} Bao-An Li,³ Wen-Qing Shen,¹ and Yin Xia^{1,4}

¹*Shanghai Institute of Applied Physics, Chinese Academy of Sciences, Shanghai 201800, China*

²*Kavli Institute for Theoretical Physics China, CAS, Beijing 100190, China*

³*Department of Physics and Astronomy, Texas A&M University-Commerce, Commerce, TX 75429-3011, USA*

⁴*University of Chinese Academy of Sciences, Beijing 100049, China*

It is well known that non-central nuclear forces, such as the spin-orbital coupling and the tensor force, play important roles in understanding many interesting features of nuclear structures. However, their dynamical effects in nuclear reactions are poorly known since only the spin-averaged observables are normally studied both experimentally and theoretically. Realizing that spin-sensitive observables in nuclear reactions may carry useful information about the in-medium properties of non-central nuclear interactions, besides earlier studies using the time-dependent Hartree-Fock approach to understand effects of spin-orbital coupling on the threshold energy and spin polarization in fusion reactions, some efforts have been made recently to explore dynamical effects of non-central nuclear forces in intermediate-energy heavy-ion collisions using transport models. The focuses of these studies have been on investigating signatures of the density and isospin dependence of the form factor in the spin-dependent single-nucleon potential. Interestingly, some useful probes were identified in the model studies while so far there is still no data to compare with. In this brief review, we summarize the main physics motivations as well as the recent progress in understanding the spin dynamics and identifying spin-sensitive observables in heavy-ion reactions at intermediate energies. We hope the interesting, important, and new physics potentials identified in the spin dynamics of heavy-ion collisions will stimulate more experimental work in this direction.

PACS numbers: 25.70.-z, 21.30.Fe, 21.10.Hw

I. INTRODUCTION

Understanding novel features of the fundamental nuclear forces and properties of strongly interacting matter under extreme conditions of density, temperature, spin, and isospin are among the main goals of nuclear physics. Heavy-ion collision (HIC) experiments play an important role in achieving these goals. Indeed, great achievements have been made using HICs at various beam energies from the sub-Colomb barrier to the highest energy available at the large hadron collider. In particular, terrestrial experiments using intermediate-energy HICs have led to strong constraints on the equations of state of hadronic matter [1] and neutron-rich nucleonic matter [2, 3].

Theoretical studies have shown recently that some spin-sensitive observables of HICs can be used to explore the in-medium properties of non-central nuclear forces. The spin-dependent nuclear interactions are important for explaining several interesting features of nuclear structure [4], such as the varying magic numbers and the shell evolution with the isospin asymmetry of finite nuclei. However, the strength, density, and isospin dependence of the nuclear spin-orbit coupling are still uncertain (see Sec. II A). Moreover, the tensor force can modify the magic number of nuclei and is an important source of the nucleon-nucleon short-range correlation. The latter is related to many interesting phenom-

ena in nuclear physics (see Sec. II B). More studies on in-medium properties of the spin-orbit coupling and tensor force are thus very much needed. HICs provide flexible ways of adjusting the conditions of the nuclear medium and may also lead to new spin-dependent phenomena. For example, the so-called “Spin Hall Effect” [5–7], which affects the dynamics of spin-up and spin-down particles differently as a result of the spin-orbit coupling, is expected to be a general feature in any spin transport process. It thus might be interesting to test if such phenomenon can also happen in HICs.

Considerable efforts using the time-dependent Hartree-Fock (TDHF) model, the spin- and isospin-dependent Boltzmann-Uehling-Uhlenbeck (SIBUU) transport model, and the quantum molecular dynamics (QMD) model have been devoted to exploring the spin dynamics in HICs (see Sec. III). Indeed, some interesting phenomena were found. For example, it was found that the inclusion of the spin-dependent nuclear interaction may affect the fusion threshold, generate the spin twist during the collision process, and lead to the spin splitting of nucleon collective flows (see Sec. III). Future comparisons with relevant experimental data may help extract properties of the in-medium spin-dependent nuclear force. Here we review briefly the main physics motivations and recent findings of studying the spin-dependent dynamics and observables in low- and intermediate-energy HICs. A major goal of this article is to stimulate more experimental work in this direction.

*Electronic address: xujun@sinap.ac.cn

II. SPIN-RELATED NUCLEAR FORCE

Based on the one-boson-exchange picture [8], nuclear force can be understood by exchanging mesons between nucleons. Exchanging the scalar σ meson and vector ω meson leads to respectively the attractive and repulsive central nuclear force as well as the spin-orbit interaction, while exchanging the π meson and ρ meson leads to respectively the long-range and short-range nuclear tensor force. Although in free space the bare nuclear force is well constrained by the nucleon-nucleon scattering data, the in-medium nuclear interactions, especially the nuclear spin-orbit interaction and tensor force, are still quite uncertain. The in-medium nuclear interactions can be studied by using microscopic many-body theories or phenomenological models, such as the non-relativistic Skyrme-Hartree-Fock (SHF) model and the relativistic mean-field (RMF) model. In the following, we will discuss the effective spin-dependent nuclear force based on the energy-density functional in the phenomenological approach.

A. Nuclear spin-orbit interaction

The nuclear spin-orbit interaction was first introduced to explain the magic numbers of nuclei [9, 10]. Nuclei with numbers of neutrons or protons equal to the magic numbers are more stable, and this reflects the special shell structure of a nucleus. Although even a simple harmonic potential leads to the shell structure of nucleon energy levels inside nuclei, the spin-orbit coupling is essential to reproduce the correct magic number.

In the Skyrme interaction, the effective spin-orbit force between two nucleons at position \vec{r}_1 and \vec{r}_2 can be expressed as [11]

$$V_{so} = iW_0(\vec{\sigma}_1 + \vec{\sigma}_2) \cdot \vec{k} \times \delta(\vec{r}_1 - \vec{r}_2)\vec{k}'. \quad (1)$$

In the above, W_0 is the spin-orbit coupling constant, $\vec{\sigma}_1$ and $\vec{\sigma}_2$ are the Pauli matrices for the two nucleons, $\vec{k} = -i(\nabla_1 - \nabla_2)/2$ is the relative momentum operator acting on the right side with ∇_1 and ∇_2 acting on the first and second nucleon, respectively, and \vec{k}' is its complex conjugate acting on the left. From the conventional Hartree-Fock method, the spin-orbit single-particle potential can be obtained based on the above effective spin-orbit force

$$U_q^{so} = \vec{W}_q \cdot (-i\nabla \times \vec{\sigma}), \quad (2)$$

where

$$\vec{W}_q = \frac{W_0}{2}(\nabla\rho + \nabla\rho_q) \quad (3)$$

is the form factor of the spin-orbit potential, with $q = n$ or p being the isospin index and ρ being the nucleon number density. Taking the operator $-i\nabla$ as the momentum \vec{p} , the right-hand side of Eq. (2) has the form

of $(\vec{r} \times \vec{p}) \cdot \vec{\sigma}$ with \vec{W}_q playing the role of \vec{r} , and this is why it is called the spin-orbit potential. By solving the Schrödinger equation with the single-nucleon Hamiltonian

$$h_q = -\nabla \cdot \left(\frac{1}{2m_q^*} \nabla \right) + U_q + U_q^{so} \quad (4)$$

with m_q^* being the effective nucleon mass and U_q being the spin-independent potential, the single-nucleon spectrum in a spherical closed-shell nucleus can be obtained.

In the RMF model, Dirac equation is solved where the spin of nucleon is treated explicitly with nucleon wave functions for different spin states [12]. The studies of SHF and RMF models on nuclear structure were reviewed in Ref. [13], and here we compare the effective spin-orbit potentials from both the relativistic and non-relativistic approach. With non-relativistic expansion of the Dirac equation, the form factor of the nucleon effective spin-orbit potential in the RMF model can be expressed in the form of [14, 15]

$$\vec{W}_{RMF} = \frac{1}{(2m - C_{eff}\rho)^2} C_{eff} \nabla\rho, \quad (5)$$

where m is the nucleon mass and the coefficient C_{eff} is related to the coupling strength and mass of the scalar σ meson and the vector ω meson, i.e.,

$$C_{eff} = \frac{g_\sigma^2}{m_\sigma^2} + \frac{g_\omega^2}{m_\omega^2}. \quad (6)$$

The form factors of the spin-orbit potential in the SHF model (Eq. (3)) and the RMF model (Eq. (5)) are different. First of all, the spin-orbit coupling strength is a constant in the SHF model, but the effective coupling strength depends on the density in the RMF model. Implementing an additional density-dependent effective nucleon-nucleon spin-orbit interaction with a coupling constant W_1 , the authors of Ref. [16] got additional contributions to the form factor as

$$\begin{aligned} \vec{W}_q^\rho &= \frac{W_1}{2} [c\rho\nabla(\rho - \rho_q) + (2+c)(2\rho_q)^c\nabla\rho_q] \\ &+ \frac{W_1}{4} c\rho^{c-1}(\rho - \rho_q)\nabla\rho, \end{aligned} \quad (7)$$

with c mimicking the density dependence. The above form was tested in Ref. [16] in a semi-infinite nuclear matter with parameters fitted to the RMF interaction. It was found that the general features of the RMF model were then reproduced with this non-relativistic density-dependent spin-orbit interaction. Nevertheless, the density dependence of the spin-orbit coupling is still largely unknown so far, and it is related to many interesting phenomena in nuclear structure studies [17–19]. Second, the spin-orbit couplings from the SHF and RMF approach have different isospin dependence, i.e., in the SHF approach the spin-orbit coupling is stronger for nucleons of the same isospin, while in the RMF approach the coupling strength is the same for neutrons and protons. This

feature impacts descriptions of properties of neutron-rich nuclei, e.g., the kink in the evolution of the charge radii for lead isotopes. It was shown that the weak isospin dependence of the spin-orbit coupling in the RMF approach can better explain the kink than the conventional SHF functional. However, if the form factor in the latter approach was modified to [20, 21]

$$\vec{W}_q = \frac{W_0}{2}(1 + \chi_w)\nabla\rho_q + \frac{W_0}{2}\nabla\rho_{q'}, \quad (q \neq q') \quad (8)$$

a similar kink can be reproduced with $\chi_w \approx 0.1$ [21], corresponding to the case with very small Fock contribution of the spin-orbit interaction. Similar efforts were made by using a modified SHF functional to reproduce the isospin dependence of the spin-orbit field in semi-infinite nuclear matter with different neutron excesses [22] and in neutron-rich nuclei [23] from a relativistic approach. In Ref. [24], the isospin dependence of the spin-orbit coupling was compared in light drip line nuclei from the relativistic mean field theory and the non-relativistic Skyrme model. Furthermore, it was observed that the commonly used Skyrme functional of the spin-orbit splitting overestimated the central density and the spin-orbit splitting of neutron drops [25], calling for new functionals of the spin-orbit coupling. The proton energy splitting of $h_{11/2}$ and $g_{7/2}$ outside the $Z = 50$ closed shell increases with neutron excess, corresponding to the decreasing strength of the nuclear spin-orbit interaction [26]. The studies so far seem to favor a weak isospin dependence of the spin-orbit coupling. However, since the isospin dependence of the spin-orbit coupling, which is important in nuclear surfaces, is often coupled with its density dependence, it is still not well settled yet.

Based on the above discussion, we proposed a general form of the form factor of the spin-orbit coupling by taking both the density and isospin dependence into account

$$\vec{W}_q = \frac{W_0}{2} \left(\frac{\rho}{\rho_0} \right)^\gamma (a\nabla\rho_q + b\nabla\rho_{q'}) \quad (q \neq q'). \quad (9)$$

The above form is artificially constructed and includes the main physics for simplicity purpose. In the above form, γ is used to mimic the density dependence of the spin-orbit coupling while fixing its strength at saturation density ρ_0 to be W_0 . a and b are parameters to vary the isospin dependence of the spin-orbit coupling, with $a = 2$ and $b = 1$ corresponding to the case of the standard SHF approach and $a = b$ corresponding to the case of the RMF approach. The values of γ , a , and b are still uncertain according to the above discussions. For the strength of the spin-orbit coupling W_0 , efforts have been made to extract its information from ground-state properties of various nuclei. Recent studies have shown that the spin-orbit coupling and the tensor force, which will be discussed in the next subsection, should be considered simultaneously to describe the spin-orbit splitting and single-nucleon spectra of nuclei. Based on the Skyrme functional and taking the uncertainties of the

tensor force into account, the strength of the spin-orbit coupling is approximately $80 - 150 \text{ MeV fm}^5$, from fitting the properties of light to heavy nuclei [27–29].

The single-nucleon Hamiltonian of Eq. (4) is adequate to describe the ground-state properties of spherical closed shell nuclei. For open shell nuclei, one needs to consider an additional spin-dependent potential using the spin-current density \vec{J} from Eq. (1)

$$U_q^J = -\frac{W_0}{2}\nabla \cdot (\vec{J} + \vec{J}_q). \quad (10)$$

\vec{J} is actually the vector component of the spin-current density tensor $J_{\mu\nu}$, see, e.g., Ref. [27] for more detailed discussions. For deformed nuclei, not only the time-even potentials (Eqs. (2) and (10)) but also the time-odd potentials should be considered [30]. Starting from the effective nucleon-nucleon spin-orbit interaction (Eq. (1)) and taking Eq. (9) into consideration, the general form of the time-even and time-odd spin-dependent potentials can be written as

$$\begin{aligned} U_q^{s\text{-even}} &= -\frac{W_0}{2} \left(\frac{\rho}{\rho_0} \right)^\gamma [\nabla \cdot (a\vec{J}_q + b\vec{J}_{q'})] \\ &\quad + \frac{W_0}{2} \left(\frac{\rho}{\rho_0} \right)^\gamma (a\nabla\rho_q + b\nabla\rho_{q'}) \cdot (\vec{p} \times \vec{\sigma}), \quad (11) \\ U_q^{s\text{-odd}} &= -\frac{W_0}{2} \left(\frac{\rho}{\rho_0} \right)^\gamma \vec{p} \cdot [\nabla \times (a\vec{s}_q + b\vec{s}_{q'})] \\ &\quad - \frac{W_0}{2} \left(\frac{\rho}{\rho_0} \right)^\gamma \vec{\sigma} \cdot [\nabla \times (a\vec{j}_q + b\vec{j}_{q'})], \quad (q \neq q') \quad (12) \end{aligned}$$

where $\vec{p} = -i\nabla$ is the momentum operator, and \vec{s} and \vec{j} are spin density and current density, respectively. We note that the time-odd potentials play an important role in the dynamics of heavy-ion reactions, which will be discussed in Sec. III.

B. Nuclear tensor force

The first strong evidence of the nuclear tensor force is from studying properties of deuterons. In the non-relativistic approach, the nuclear tensor force between two nucleons at position \vec{r}_1 and \vec{r}_2 is often expressed with the tensor operator written as

$$S_{12} = 3 \frac{(\vec{\sigma}_1 \cdot \vec{r})(\vec{\sigma}_2 \cdot \vec{r})}{r^2} - (\vec{\sigma}_1 \cdot \vec{\sigma}_2), \quad (13)$$

where $\vec{r} = \vec{r}_1 - \vec{r}_2$ is the relative position vector. One thus sees that whether the tensor force is attractive or repulsive depends on the relative direction between the spin and the relative position vector, i.e., $S_{12} > 0$ for $\vec{\sigma}_{1(2)}$ parallel to \vec{r} and $S_{12} < 0$ for $\vec{\sigma}_{1(2)}$ perpendicular to \vec{r} .

The tensor term in the effective nuclear interaction was first included in the Skyrme force [31], but afterwards it

was neglected due to its complex form. Recently it attracted renewed interests. It has been found by Otsuka *et al.* that the nuclear tensor force may affect the shell structure or even modify the magic number of nuclei [32–34]. The combined effects of the spin-orbit coupling and the nuclear tensor force sometimes hamper our understanding on both of them [35, 36]. Based on the random phase approximation, effects of the tensor force on the multipole response of magic nuclei have been studied, and a large effect on the magnetic dipole states was observed [37]. Besides, it was proposed that the spin-isospin excitation of finite nuclei may serve as a useful observable to assess the strength of the tensor force [38, 39]. The existence of the tensor force may also open a shell gap for large neutron numbers, having a consequent implication for the synthesis of neutron-rich superheavy elements [40].

Although the nuclear tensor force has no effect on the equation of state of spin-saturated nuclear matter based on the studies at mean-field level, it affects the properties of nuclear matter from many-body calculation beyond the mean field. It was found that the repulsive central force and the tensor force are two important sources of nucleon-nucleon short-range correlation [41]. The high-momentum tail of nucleon distribution in nuclear matter as well as in finite nuclei was observed even at zero temperature based on these studies [42–45]. Great efforts have been made in measuring the short-range nucleon-nucleon correlation and extracting the ratio of nucleons in the high-momentum tail experimentally [46–50] and theoretically [51, 52], see, e.g., Ref. [53] for a review. In particular, it was found that the neutron-proton correlation is much stronger than the correlation between neutron-neutron and proton-proton pairs [48–50], and this is mainly due to the nuclear tensor force. The isospin dependence of the short-range correlation can lead to interesting consequences, such as the reduction of the kinetic contribution to the nuclear symmetry energy [54–56] compared to the free Fermi gas scenario. Since the symmetry energy at saturation density is constrained to be around 30 MeV from many analyses, see, e.g., Ref. [57], the isospin-dependent short-range correlation effectively increases the potential contribution to the symmetry energy and thus the symmetry potential effect, which may lead to enhanced isospin effects in intermediate-energy HICs [58, 59].

III. SPIN IN NUCLEAR REACTIONS

The spin hall effect was first predicted by M.I. Dyakonov and V.I. Perel in 1971 [6, 7], while the term "Spin Hall Effect" was named by Hirsch in 1999 [5]. Considering the transport of spin-up and spin-down particles with spin-orbit coupling, i.e., $U^{so} = -\vec{L} \cdot \vec{\sigma}$ with \vec{L} being the angular momentum and $\vec{\sigma}$ being the particle spin, the spin-up (spin-down) particles tend to turn left (right) to couple with the angular momentum and lower the energy,

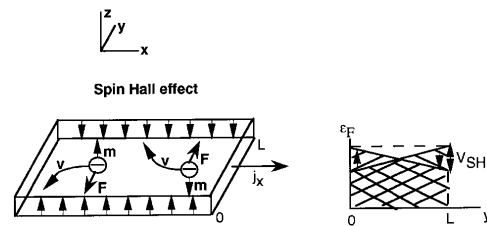


FIG. 1: Cartoon illustrating the spin hall effect. Taken from Ref. [5].

leading to the splitting of final observables for different spin states, as shown in Fig. 1. In this section, we will discuss similar effects in low- and intermediate-energy HICs based on the framework of TDHF, BUU, and QMD, with more complicated forms of spin-orbit coupling from spin-dependent nuclear interactions.

A. TDHF model study

The mean-field dynamics of nucleons in the TDHF model is described by

$$i \frac{\partial}{\partial t} \phi_i = h \phi_i, \quad (14)$$

where ϕ_i is the wave function of the i th nucleon and the single-nucleon Hamiltonian is given by

$$h \phi_i = \frac{\delta E}{\delta \phi_i^*}, \quad (15)$$

with E being the energy functional of the nuclear system from Hartree-Fock calculation. The single-nucleon Hamiltonian is generally a function of nucleon number density ρ , spin density \vec{s} , current density \vec{j} , spin-current density \vec{J} , and so on, and their definitions in terms of the nucleon wave function are

$$\rho = \sum_i \phi_i^* \phi_i, \quad (16)$$

$$\vec{s} = \sum_i \sum_{\sigma, \sigma'} \phi_i^* \langle \sigma | \vec{\sigma} | \sigma' \rangle \phi_i, \quad (17)$$

$$\vec{j} = \frac{1}{2i} \sum_i (\phi_i^* \nabla \phi_i - \phi_i \nabla \phi_i^*), \quad (18)$$

$$\vec{J} = \frac{1}{2i} \sum_i \sum_{\sigma, \sigma'} (\phi_i^* \nabla \phi_i - \phi_i \nabla \phi_i^*) \times \langle \sigma | \vec{\sigma} | \sigma' \rangle, \quad (19)$$

with $\langle \sigma | \vec{\sigma} | \sigma' \rangle$ being the pauli matrix element. Numerically, these densities can be calculated on the coordinate space grid and Eq. (14) can be solved with a fixed time step. For more details, we refer the reader to Refs. [60, 61]. The TDHF framework works well for low-energy heavy-ion reactions and in studying resonances dynamics.

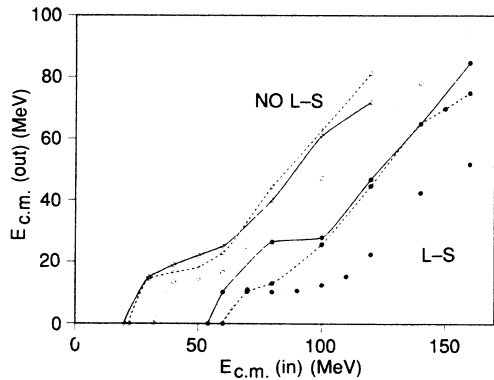


FIG. 2: The relation between the out-going energy and incoming energy in $O^{16} + O^{16}$ reaction from TDHF study. The filled (open) circles are results with (without) spin-orbit force, and the solid, dashed, and dotted curves represent results from three different Skyrme forces. Taken from Ref. [63].

In the old calculations, the single-nucleon Hamiltonian was generally calculated from the SHF model without the spin-orbit interaction and time-odd terms. The spin-orbit force was first introduced to the TDHF framework in Refs. [62–64]. It is interesting to see that the spin-orbit force enhances the dissipation in the fusion reaction and transforms the relative motions of the two nuclei into the internal excitations. The fusion threshold energy in $O^{16} + O^{16}$ reaction is increased by about a factor of 2 [62, 63], as shown in Fig. 2 with three different parameterizations of Skyrme force. The fusion cross section obtained from TDHF calculation was increased after including the spin-orbit force [62].

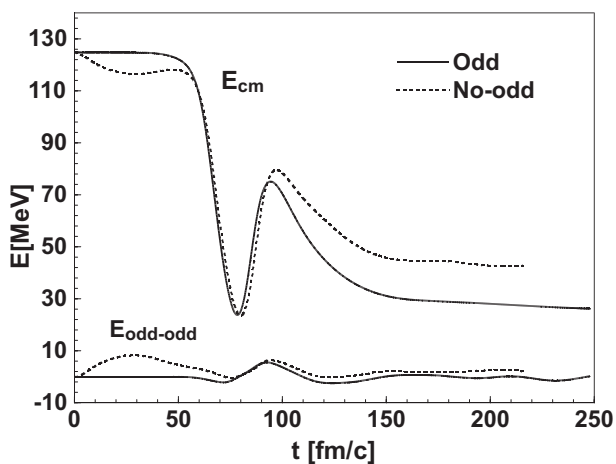


FIG. 3: Center-of-mass energy evolution in central $O^{16} + O^{16}$ reaction with (solid lines) and without (dashed lines) time-odd contributions from TDHF calculation. The time window of the reaction process is from about 50 fm/c to 120 fm/c. Taken from Ref. [65].

With only time-even contribution of the spin-orbit interaction, i.e., the spin-orbit potential (Eq. (2)) and the

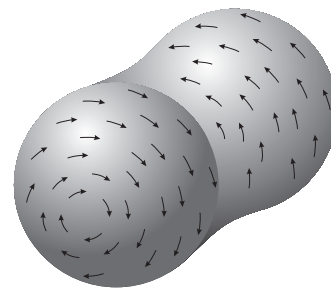


FIG. 4: Spin excitation in central $O^{16} + O^{16}$ reactions from TDHF study with both time-even and time-odd terms. Taken from Ref. [65].

potential with spin-current density \vec{J} (Eq. (10)), spurious spin twist can be generated in a free moving nucleus, as a result of spin-orbit coupling. Obviously, this phenomena is not reasonable as it depends on the reference frame. Considering that all kinds of collision geometry can be realized in HICs, the time-odd terms were further introduced in the TDHF calculation in Refs. [65, 66] to satisfy the invariance under Galilei transformations. It is seen from Fig. 3 that there is no such spurious spin and the kinetic energy is a constant before 50 fm/c when the nuclei are moving freely, as a result of suppression effect on the time-even terms from the time-odd terms. During the reaction process, the real spin twist appears due to the overwhelming effect of the time-odd terms on the time-even terms, as shown in Fig. 4. At the end of the reaction, the energy of outgoing nuclei is smaller with the time-odd terms as shown in Fig. 3, indicating a stronger dissipation. Besides the spin excitation, it was found that the fusion description was further improved with the time-odd terms and the spin-current pseudotensor contribution [66]. A more detailed study on this topic was done recently [67], where it was found that the dissipation is dominated by the time-even contribution of the spin-orbit force at lower energies but by the time-odd terms at higher energies.

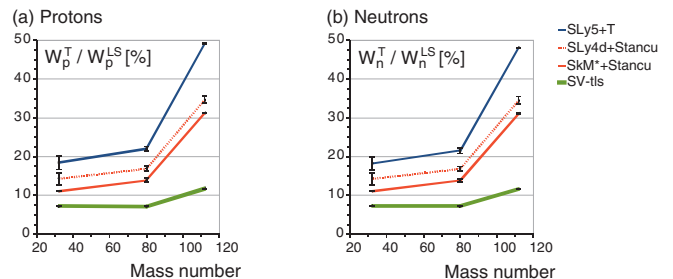


FIG. 5: (Color online) Ratios of the spin mean field from the spin-current density representing the tensor force to that from the spin-orbit force for protons (left) and neutrons (right) as a function of the mass of reaction nuclei. Different parameterizations of the Skyrme force are used in the study. Taken from Ref. [68].

Besides the spin-orbit force, the additional contribution of the spin-current density \vec{J} was introduced in the TDHF calculation representing the contribution from the tensor force in Ref. [68]. It was found that the dissipation effect from the tensor force is small compared with that from the spin-orbit force [68, 69]. However, the spin mean field can be enhanced with the nuclear tensor force, and the enhancement becomes important with the increasing mass of the colliding nuclei, as shown in Fig. 5, depending on the parameterization of the Skyrme force. A more complete study by including the full Skyrme functional as well as the tensor force in the TDHF calculation was done very recently in Ref. [70]. It was found that the Skyrme tensor force has non-negligible effects on low-energy heavy-ion dynamics and the fusion threshold energy.

B. BUU model study

The TDHF model works well in low-energy HICs, while the particle emission and nucleon-nucleon scattering are still lacking. To describe these effects in intermediate-energy HICs, BUU models and QMD models are suitable candidates. In the BUU framework, the Boltzmann equation is solved with test particle method [71, 72]. In the previous studies, an isospin-dependent BUU (IBUU) transport model has been used to describe the isospin dynamics in intermediate-energy HICs [3]. Recently, the spin degree of freedom of nucleons and the spin-orbit interaction were incorporated in the IBUU model, and the new model is dubbed as the spin- and isospin-dependent BUU (SIBUU) model [73–77]. In this section, we summarize the main results published originally in Refs. [73–77].

In the SIBUU model, each nucleon is assigned randomly a unit vector representing the expectation value of its spin. In this way, the spin projection of each nucleon at arbitrary direction can be easily calculated. In the transport simulation, z direction is set as the beam momentum and x direction is for the impact parameter. Since the total angular momentum in non-central HICs is in the y direction perpendicular to the reaction plane, i.e., $x - o - z$ plane, it is reasonable to study the spin polarization in y direction. We thus determine the nucleons with spin projection on $+y$ ($-y$) direction as the spin-up (spin-down) nucleons.

Considering the general form of the time-even and time-odd spin-dependent potentials in Eqs. (11) and (12), the time evolutions of the coordinate, momentum, and

spin degree of freedom are described by

$$\frac{d\vec{r}}{dt} = \frac{\vec{p}}{m} + \frac{W_0}{2} \left(\frac{\rho}{\rho_0} \right)^\gamma \vec{\sigma} \times (a\nabla\rho_q + b\nabla\rho_{q'}) - \frac{W_0}{2} \left(\frac{\rho}{\rho_0} \right)^\gamma \nabla \times (a\vec{s}_q + b\vec{s}_{q'}), \quad (20)$$

$$\frac{d\vec{p}}{dt} = -\nabla U_q - \nabla U_q^{s-even} - \nabla U_q^{s-odd}, \quad (21)$$

$$\frac{d\vec{\sigma}}{dt} = W_0 \left(\frac{\rho}{\rho_0} \right)^\gamma [(a\nabla\rho_q + b\nabla\rho_{q'}) \times \vec{p}] \times \vec{\sigma} - W_0 \left(\frac{\rho}{\rho_0} \right)^\gamma [\nabla \times (a\vec{j}_q + b\vec{j}_{q'})] \times \vec{\sigma}. \quad (22)$$

One sees that the three degrees of freedom couple with each other. The number density ρ , the spin density \vec{s} , the current density \vec{j} , and the spin-current density \vec{J} are calculated from test particle method [71, 72, 74]. Since the mixing of the long-range Fock contribution and the spin interaction is a complex problem, the momentum dependence is not included in the spin-independent potential U_q for the moment. In addition, the spin of nucleons are randomized after nucleon-nucleon scatterings, by approximately taking the spin flip effect into consideration [78, 79].

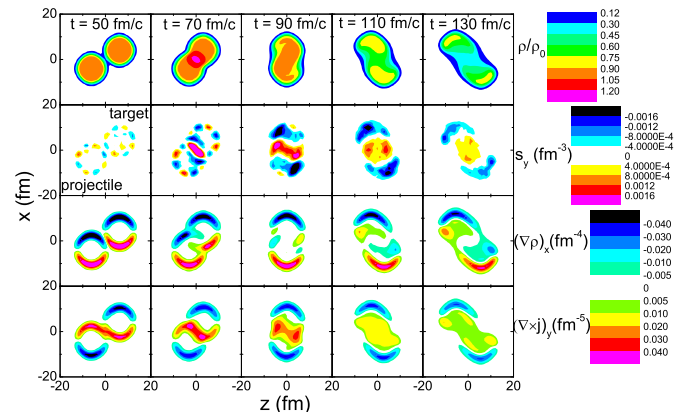


FIG. 6: (Color online) Time evolution of contours of reduced number density ρ/ρ_0 , y component of the spin density s_y , x component of the number density gradient $(\nabla\rho)_x$, and y component of the curl of the current density $(\nabla \times \vec{j})_y$ in non-central Au+Au collision at the beam energy of 50 MeV. Taken from Ref. [73].

The time evolution of relevant density contours from SIBUU calculation are displayed in Fig. 6. The gradient of number density $\nabla\rho$ and the curl of the current density \vec{j} show the strength of the time-even and time-odd spin-dependent potential, respectively, and both of them are closely related to the evolution of the number density shown in the first row of Fig. 6. The nucleon spin tends to be parallel to $\vec{p} \times \nabla\rho$ from the time-even potential (Eq. (11)), while it tends to be parallel to $\nabla \times \vec{j}$ from the time-odd potential (Eq. (12)). The contributions from

the time-even and time-odd potentials are opposite to each other. One sees that before the two nuclei touch each other there is no spin polarization as a result of the cancellation of the time-even and time-odd potentials, consistent with the findings from TDHF studies. During the collision process, the participant is polarized in the $+y$ direction, i.e., in the direction of the total angular momentum, following the preference direction of the time-odd potential. It is seen that the direction of the spin polarization is consistent with that in Fig. 4 from TDHF calculation with both time-even and time-odd potentials.

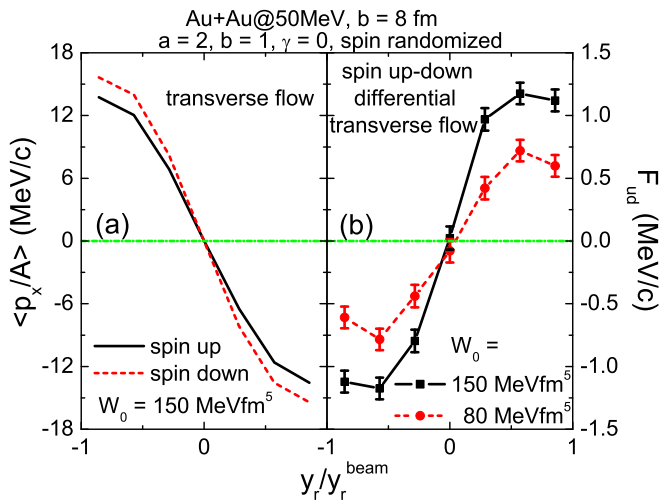


FIG. 7: (Color online) Transverse flow of spin-up and spin-down nucleons (left) and spin up-down differential transverse flow (right) with different strength of the spin-orbit coupling in non-central Au+Au collisions at the beam energy of 50 MeV. Taken from Ref. [73].

Transverse flow is one of the most important observables for extracting the equation of state of produced matter and studying the nuclear interaction in HICs [1, 72, 80]. The left panel of Fig. 7 displays the transverse flow of spin-up and spin-down nucleons as a function of reduced rapidity y_r/y_r^{beam} . We note that the target (projectile) nucleus is in the $+x$ ($-x$) direction in Fig. 6, which is different from the conventional initialization, leading to the negative slope of the transverse flow. However, this doesn't prevent the reader from seeing the obvious splitting of transverse flow between spin-up and spin-down nucleons. With a detailed orientation analysis, one can find that again the time-odd potential dominates the effect, giving the spin-up (spin-down) nucleons an attractive (repulsive) potential. This can be understood in a naive picture that the spin-up (spin-down) nucleons parallel (antiparallel) to the direction of total angular momentum and thus feel an attractive (repulsive) potential. One can further define the spin up-down

differential transverse flow as follows

$$F_{ud}(y_r) = \frac{1}{N(y_r)} \sum_{i=1}^{N(y_r)} \sigma_i(p_x)_i, \quad (23)$$

where σ_i is 1 for spin-up nucleons and -1 for spin-down nucleons, and $N(y_r)$ is the number of nucleons at rapidity y_r . The above spin up-down differential transverse flow largely cancels the effect from the spin-independent nuclear interaction while preserves the information of the spin-dependent potential. Indeed, the slope of F_{ud} increases with increasing spin-orbit coupling constant, indicating that it is a good probe of nuclear spin-dependent interaction.

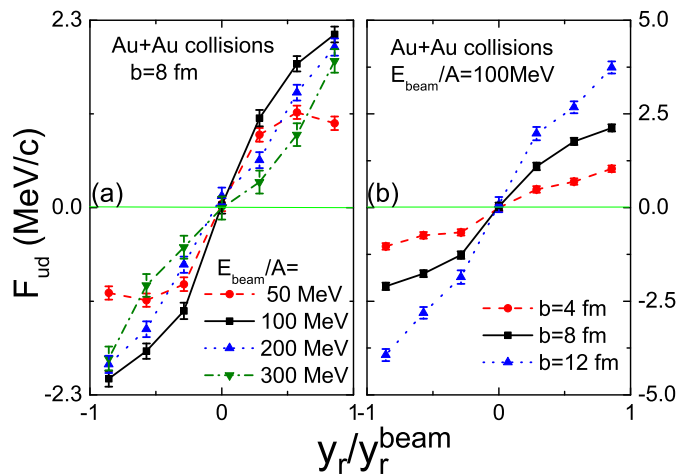


FIG. 8: (Color online) Dependence of the spin up-down differential transverse flow on the beam energy (left) and the impact parameter (right) in non-central Au+Au collisions. Taken from Ref. [74].

The spin up-down differential transverse flow was further analyzed in detail in Ref. [74]. Figure 8 displays the dependence of F_{ud} on the beam energy and the centrality. At higher beam energies, the angular momentum is larger while the nucleon-nucleon scattering is more violent, with the former enhancing the spin-dependent potential while the latter washing out part of the information of spin dynamics. The competition leads to a maximum slope of F_{ud} at the beam energy of about 100 MeV, as shown in the left panel of Fig. 8. Since the spin-dependent potential is related to the density gradient and is thus a surface effect, the slope of F_{ud} increases with the increasing value of the impact parameter, as shown in the right panel of Fig. 8.

In the neutron-rich collision system where the relevant neutron densities are larger than proton densities, the difference of the spin up-down differential transverse flow of neutrons and protons can be useful to probe the isospin-dependence of the spin-orbit coupling in HICs. The analysis was carried out with a stronger isospin-like coupling ($a = 2, b = 1$) and a stronger isospin-unlike coupling

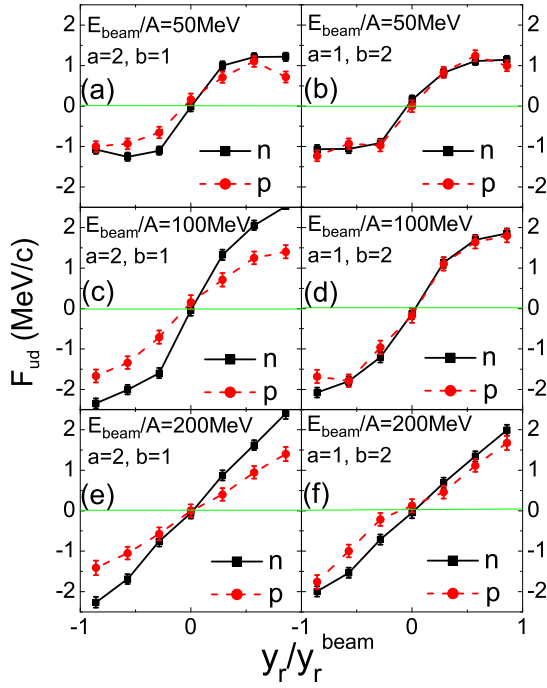


FIG. 9: (Color online) Spin up-down differential transverse flow of neutrons and protons at different beam energies and with two typical isospin dependence of the spin-orbit coupling. Taken from Ref. [74].

($a = 1, b = 2$), and the resulting F_{ud} were calculated at different beam energies shown in Fig. 9. A stronger isospin-like spin-orbit coupling, which is exactly the case of SHF interaction, leads to a larger F_{ud} for neutrons than for protons, while a stronger isospin-unlike coupling gives opposite predictions or similar F_{ud} for neutrons and protons. The effect is appreciable from beam energy 50 MeV to 200 MeV, while the beam energy of 100 MeV is the optimized one due to the largest magnitude of F_{ud} .

The density dependence of the spin-orbit coupling has bothered many nuclear physicists and hampered the understanding of nuclear spin-orbit interaction in nuclear structure studies. Since HICs have the advantage of constructing the system with designed density, isospin, and momentum current, it might be helpful in extracting useful information of the density dependence of the spin-orbit coupling. As is known, nucleons of high transverse momentum (p_T) emit early from the high-density phase in HICs, and the density of the high-density phase increases with increasing beam energy. This feature can be used to extract the density dependence of the spin-orbit coupling, as illustrated in Fig. 10. Without high- p_T cut, the slope of F_{ud} can hardly be distinguished as shown in the left panel of Fig. 10, because nucleon emission from low-density phase, which is similar at different beam energies, dominates the results. With high- p_T cut, the slope of F_{ud} is smaller at lower collision energies but larger at higher collision energies from a linearly increas-

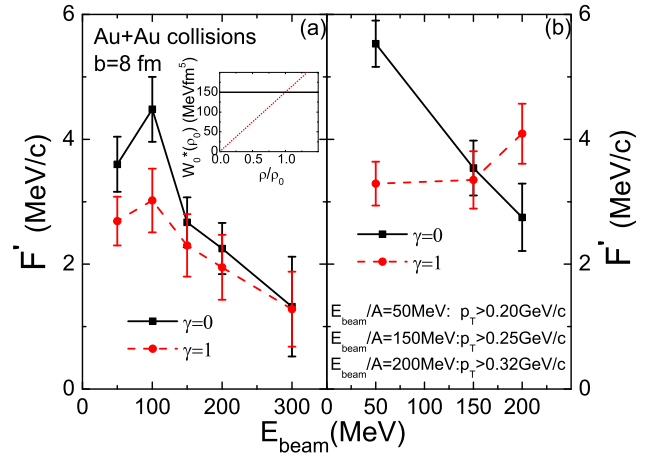


FIG. 10: (Color online) Slope parameter of the spin up-down differential transverse flow F' without (left) and with (right) high transverse momentum cut from different density dependence of the spin-orbit coupling at different beam energies. Taken from Ref. [74].

ing spin-orbit coupling strength, compared to the case with a constant one. In this way, the strength and the density dependence of the spin-orbit coupling can be disentangled.

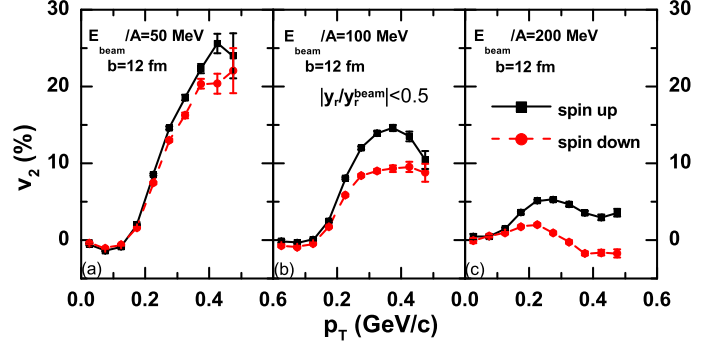


FIG. 11: (Color online) Transverse momentum dependence of the elliptic flow of mid-rapidity nucleons in peripheral Au+Au collisions at different beam energies. Taken from Ref. [75].

In non-central HICs, the azimuthal distribution of emitted nucleons can always be expressed as

$$E \frac{d^3 N}{dp^3} = \frac{d^2 N}{2\pi p_T dp_T dy_r} [1 + 2v_1(y_r, p_T) \cos(\phi) + 2v_2(y_r, p_T) \cos(2\phi) + \dots] \quad (24)$$

with $\phi = \tan^{-1}(p_y/p_x)$ being the azimuthal angle, and $v_1 = \langle \cos(\phi) \rangle$ and $v_2 = \langle \cos(2\phi) \rangle$ are called the directed flow and elliptic flow, respectively. The directed flow is similar to the transverse flow but it depends on the flow angle rather than magnitude. The elliptic flow is

positive at lower energies, negative at intermediate energies, and becomes positive again at higher energies. The positive elliptic flow means more particles move in-plane than out-of-plane as a result of hydrodynamics, while the negative elliptic flow is a result of the squeeze-out effect on the expansion of participant matter by the spectator nucleons [1]. Despite of the complicated dynamics, the elliptic flow serves as a useful probe of the properties of nuclear matter formed in HICs and the nuclear interaction. The transverse momentum dependence of v_2 of spin-up and spin-down nucleons at mid-rapidity is displayed in Fig. 11. Except for the different behaviors of v_2 at different beam energies, the large elliptic flow of spin-up nucleons than spin-down nucleons is observed, especially at higher transverse momentum as a result of the stronger spin-orbit coupling for energetic nucleons. At the energy range considered, a more attractive mean-field potential leads to a larger v_2 in peripheral HICs, consistent with the effect of spin-dependent potential on the spin splitting of transverse flow discussed above.

The above observables are for free nucleons. Experimentally it is easier to detect charged particles rather than neutrons, leading to difficulties of measuring the spin splitting of transverse flows for protons and neutrons and identifying the isospin dependence of the spin-orbit coupling. Of course the spin measurement is another challenge which will be discussed in the next section. Once the corresponding detectors are set up, the spin splitting of observables for charged light clusters may be more easily measured. For transport models with point-like particles, the dynamical coalescence approach has been shown to be successful in studying the hadronization in relativistic HICs [81, 82] and light cluster formation in intermediate-energy HICs [83, 84]. In this approach, the probability for nucleons to form a light cluster is proportional to the nucleon Wigner function of the light cluster [83, 84], and the proportional constant is the statistical factor determined by the spin-isospin degeneracy. For example, with explicitly knowing the isospin of nucleons, the statistical factor for a neutron and a proton to form a deuteron is $3/8$, while that for one neutron and two protons to form a ${}^3\text{He}$ is $1/12$. Since now the spin of each nucleon is also explicitly known, the dynamical coalescence can be further improved by considering the antisymmetrization of the product of spin and isospin wave function. For example, the statistical factor for a spin-up neutron and a spin-up proton to form a spin-up deuteron is $1/2$, while for a spin-up neutron, a spin-up proton, and a spin-down proton to form a spin-up ${}^3\text{He}$ is $1/2$. This improvement has been applied to study spin splitting observables for deuterons, tritons, and ${}^3\text{He}$ [85]. It has been checked that after spin average the results reproduce those without explicit spin treatment.

Figure 12 displays the spin splitting of the directed flows for deuterons, tritons, and ${}^3\text{He}$ in non-central Au+Au collisions at the beam energy of 100 MeV. The directed flow of spin-down clusters is larger than that of spin-up ones. The spin splitting of the directed flow is

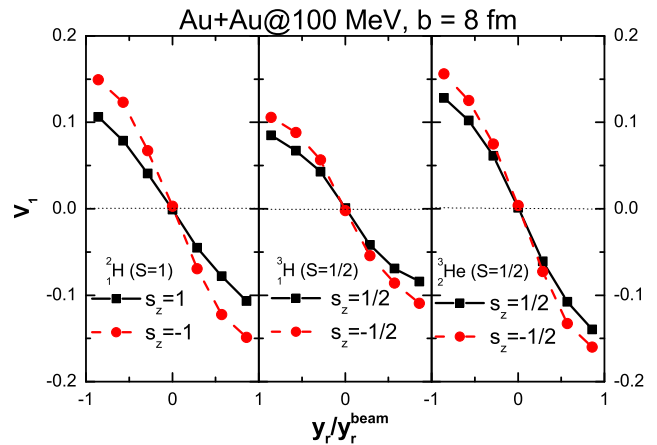


FIG. 12: (Color online) Directed flow of deuteron, triton, and ${}^3\text{He}$ of different spin states in non-central Au+Au collisions at the beam energy of 100 MeV. s_z represents the spin state projecting on the y direction perpendicular to the reaction plane. Taken from Ref. [85].

largest for deuterons due to its large spin quantum number, i.e., $S = 1$. The spin splitting observables of tritons and ${}^3\text{He}$ might be more easily measurable for extracting the isospin dependence of the spin-orbit coupling experimentally.

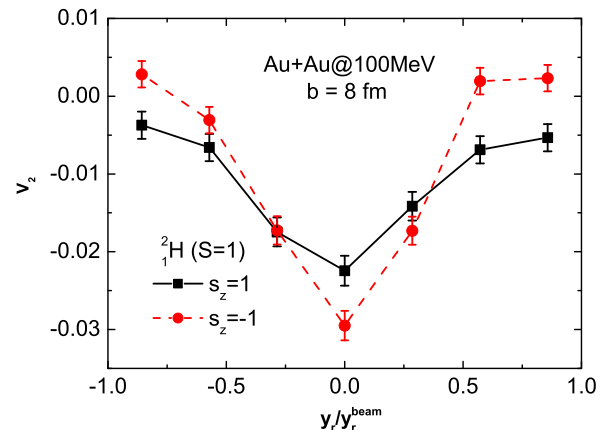


FIG. 13: (Color online) Elliptic flow of spin-up and spin-down deuterons in non-central Au+Au collisions at the beam energy of 100 MeV. s_z represents the spin state projecting on the y direction perpendicular to the reaction plane. Taken from Ref. [85].

The elliptic flow of different spin states of deuterons has been illustrated in Fig. 13, in non-central Au+Au collisions at the beam energy of 100 MeV. It is seen that the elliptic flow of spin-down deuterons is more negative at mid-rapidity, but is slightly positive at large rapidity, indicating an obvious spin splitting even taking the statistical error into account. Again, the magnitude of the v_2 as well as its spin splitting for deuterons is larger than

that of free nucleons according to Ref. [75], and might serve as a better spin-dependent observable.

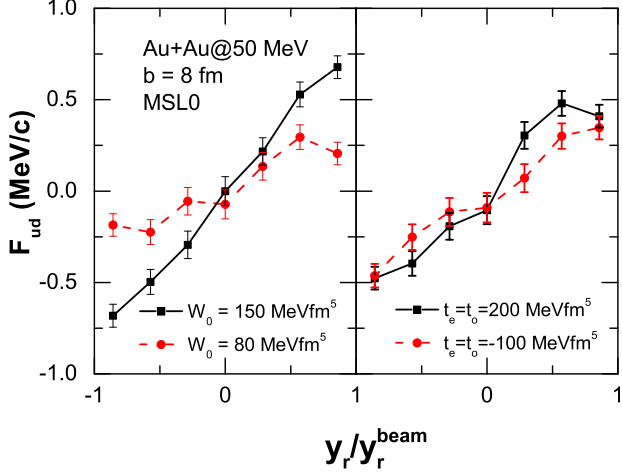


FIG. 14: (Color online) Spin up-down differential transverse flow from full Skyrme calculation using MSL0 force without (left) and with tensor force (right). Taken from Ref. [85].

Further preliminary calculation with full Skyrme functional has been done. A standard Skyrme functional with MSL0 parameterization [86] has been used in the calculation. The detailed derivation and expression of full Skyrme functional with both time-even and time-odd terms can be found in Refs. [27, 29, 30]. The resulting spin up-down differential transverse flow is shown in the left panel of Fig. 14. One can see the similar sensitivity of F_{ud} to the spin-orbit coupling strength although the magnitude is a little smaller, compared to the result shown in Fig. 7 where only the spin-orbit coupling is applied. To investigate the effect of nuclear tensor force on the spin dynamics of intermediate-energy HICs, a zero-range tensor force of the form

$$\begin{aligned}
 v_t(\vec{r}) = & \frac{t_e}{2} \{ [3(\vec{\sigma}_1 \cdot \vec{k}')(\vec{\sigma}_2 \cdot \vec{k}') - (\vec{\sigma}_1 \cdot \vec{\sigma}_2)k'^2] \delta(\vec{r}) \\
 & + \delta(\vec{r}) [3(\vec{\sigma}_1 \cdot \vec{k})(\vec{\sigma}_2 \cdot \vec{k}) - (\vec{\sigma}_1 \cdot \vec{\sigma}_2)k^2] \} \\
 & + t_o [3(\vec{\sigma}_1 \cdot \vec{k}')\delta(\vec{r})(\vec{\sigma}_2 \cdot \vec{k}) - (\vec{\sigma}_1 \cdot \vec{\sigma}_2)\vec{k}' \cdot \delta(\vec{r})\vec{k}]
 \end{aligned} \quad (25)$$

is incorporated to the full Skyrme transport model calculation, where $\vec{r} = \vec{r}_1 - \vec{r}_2$ is the relative coordinate, \vec{k} and \vec{k}' are the relative momentum operator and its complex conjugate, respectively, and t_e and t_o are the triplet-even and triplet-odd strength parameter. The energy density function derived from the above tensor force can be found in Refs. [27, 29], where the corresponding terms (such as the spin-current density \vec{J}) are non-negligible only when local spin polarization is produced. The resulting spin up-down differential transverse flow is shown in the right panel of Fig. 14. It is seen that the slope of F_{ud} is not

very sensitive to the values of t_e or t_o unless extremely large coupling constant is used. This feature is consistent with TDHF study where the spin dynamics is dominated by the spin-orbit coupling. However, one would expect that with spin-polarized beam or target, the tensor force effect can be much enhanced.

C. QMD model study

In the QMD framework, the Wigner function of each nucleon is treated as Gaussian wave packet in both coordinate and momentum space [87, 88], and the two-nucleon interaction is related to the effective two-body interaction and the overlap of their wave functions. The equation of motion in the QMD model is given by the semiclassical canonical equation, i.e.,

$$\begin{aligned}
 \frac{d\vec{r}}{dt} &= \nabla_p H, \\
 \frac{d\vec{p}}{dt} &= -\nabla_r H,
 \end{aligned} \quad (26)$$

where \vec{r} and \vec{p} are respectively the central coordinate and momentum of the wave packet, and H is the Hamiltonian of the system including the kinetic and potential energy.

In a recent study, the nuclear spin-orbit interaction was incorporated to the ultra-relativistic QMD (UrQMD) model. The potential energy contribution of the spin-orbit interaction is expressed as [89]

$$U_s = \int u_s d^3r, \quad (27)$$

where the spin-dependent potential u_s consists of the time-even and time-odd contribution written as

$$\begin{aligned}
 u_s^{even} &= -\frac{W_0}{2} (\rho \nabla \cdot \vec{J} + \rho_n \nabla \cdot \vec{J}_n + \rho_p \nabla \cdot \vec{J}_p), \quad (28) \\
 u_s^{odd} &= -\frac{W_0}{2} [\vec{s} \cdot (\nabla \times \vec{j}) \\
 & + \vec{s}_n \cdot (\nabla \times \vec{j}_n) + \vec{s}_p \cdot (\nabla \times \vec{j}_p)], \quad (29)
 \end{aligned}$$

where W_0 represents the spin-orbit coupling strength, and ρ , \vec{s} , \vec{j} , and \vec{J} are the number, spin, current, and spin-current densities, which can be calculated from local Wigner function of the nucleon [89].

The spin dynamics was analyzed based on the above framework. Similar spin splittings of the directed flow and the elliptic flow were observed in non-central Au+Au collisions at the beam energy of 150 MeV, as shown in Fig. 15. It was argued that the net spin-dependent potential is attractive for spin-up protons and repulsive for spin-down protons, leading to a larger directed flow for spin-down protons than spin-up protons. The spin splitting of p_T -integrated elliptic flow was found to be small and only visible in peripheral collisions, and it was found that v_2 for spin-down protons is slightly larger than that for spin-up ones. Since the conventional initial direction

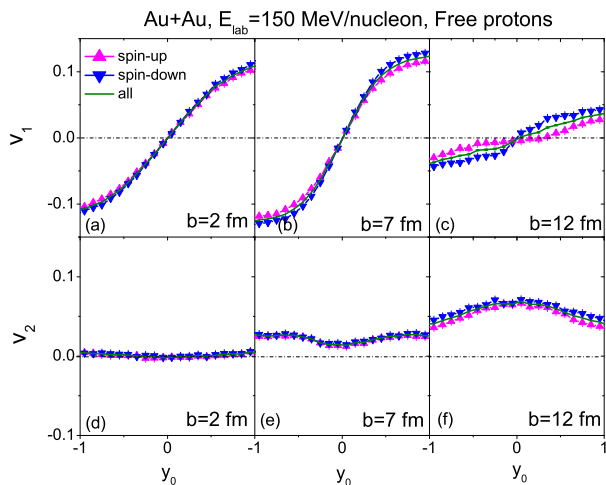


FIG. 15: (Color online) The directed flow (upper panels) and elliptic flow (lower panels) for spin-up and spin-down protons in non-central Au+Au collisions at the beam energy of 150 MeV from QMD calculation. Taken from Ref. [89].

of the target and projectile is used as shown in Fig. 3 of Ref. [89], the spin-up (spin-down) nucleons correspond to the spin-down (spin-up) ones in the SIBUU study [73–77]. Although the spin splitting of final collective flow is a robust phenomenon in both models, further studies are needed to understand the relative sign of the splitting.

Analysis was further done on the beam energy dependence of the flow splitting. Defining κ_{up} and κ_{down} as the slope parameter of the directed flow of spin-up and spin-down protons, the slope difference is shown to increase with increasing impact parameter, as shown in the upper panel of Fig. 16, qualitatively consistent with SIBUU studies. In non-central Au+Au collisions, it was found that the slope difference first increases then decreases with increasing beam energy, and the maximum difference appears at the beam energy of 150 MeV, similar to the finding in the SIBUU model where the maximum slope of the spin up-down differential transverse flow appears at the beam energy of about 100 MeV.

It was further emphasized in Ref. [89] that the spin averaged flow results do not change after including the spin-orbit interaction, as a result of the cancellation of spin-up and spin-down nucleons. In addition, the spin splitting of the flow slope caused by the spin-orbit interaction is comparable to the isospin splitting caused by the nuclear symmetry energy, especially for neutrons. These findings are all consistent with the observations in SIBUU studies [73–77].

IV. EXPERIMENTAL STATUS

Due to the difficulties of spin measurement in HIC experiments, the main focus in the past is mainly on the spin-averaged observables, so that the information

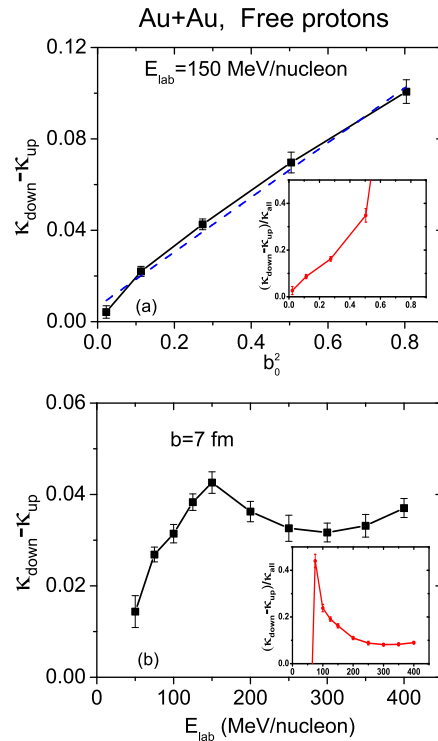


FIG. 16: (Color online) The difference of the slope of directed flow between spin-up and spin-down protons as a function of impact parameter (upper panel) and beam energy (lower panel). The dashed line in the upper panel is a linear fit, while the inset in the lower panel shows the relative difference. Taken from Ref. [89].

of spin dynamics is neglected. Thanks to the great efforts made by experimental nuclear physicists, the measurements of the spin of free nucleons and light clusters now become possible. Although the detailed experimental status will be presented in another topic review of this issue, here we'd like to briefly mention two related experiments that might be relevant in analyzing the probes discussed above. One of them is the spin-polarized beam which can be produced through pick-up or removal reactions at Rikagaku Kenkyusho (RIKEN) [90, 91], Gesellschaft für Schwerionenforschung mbH (GSI) [92], the National Superconducting Cyclotron Laboratory (NSCL) [93], and the Grand Accélérateur National d'Ions Lourds (GANIL) [94–96]. It is expected that the effects of spin dynamics with spin-polarized beam will be much enhanced, providing a better system for extracting the information of the spin-dependent nuclear force, especially the nuclear tensor force. For the spin-excitation state of heavy clusters, the spin polarization and alignment can be measured via the angular distribution of its γ or β decay, see, e.g., Ref. [97] for a review. Making use of the analyzing power of a nucleus might be the most promising way of identify-

ing the spin of free nucleons or light clusters experimentally. The analyzing power indicates the left-right scattering asymmetry of an incident polarized nucleon on the target nucleus. The spin-dependent scattering is a result of the interference of electromagnetic interaction and hadronic force [98], and the spin flip is observed between not only charged-charged scatterings but also charged-neutral scatterings. It is noteworthy that at certain energies and scattering angles the analyzing power can be as large as 100% [99]. Experimental efforts are thus encouraged by using the selected nucleus as a 'detector' whose analyzing power is known in prior. In this way the spin of corresponding particles can be measured and the probes discussed in the previous sections can be analyzed.

V. SUMMARY

In summary, we outlined the major physics motivations of investigating the in-medium spin-dependent nuclear interactions, i.e., the spin-orbit interaction and the nuclear tensor force, and summarized some recent efforts in exploring the spin dynamics in low- and intermediate-energy heavy-ion collisions. In particular, the studies on the strength, the density, and the isospin dependence of the spin-orbit interaction as well as the short-range correlation induced by the tensor force are highlighted. In TDHF studies, it has been found that the spin-orbit interaction can enhance the dissipation in low-energy heavy-ion reactions and increase the fusion threshold. Incorporating both the time-even and time-odd contribution of the spin-orbit interaction can lead to nontrivial spin polarization, while the tensor force slightly enhances

the spin field compared to the spin-orbit interaction. In the studies using HICs at intermediate energies, both the spin- and isospin-dependent BUU model and QMD model predict the spin splitting of the nucleon collective flow, which seems to be a robust phenomenon. In the BUU model studies, efforts have been made in extracting the isospin dependence of the spin-orbit coupling and disentangle its strength and density dependence. Preliminary results on spin splitting of observables related to the light clusters and those from full Skyrme calculation with nuclear tensor force have also been discussed in the BUU model studies. We hope the findings summarized in this review will soon stimulate more experimental work in this direction.

Acknowledgments

This work was supported by the Major State Basic Research Development Program (973 Program) of China under Contract Nos. 2015CB856904 and 2014CB845401, the National Natural Science Foundation of China under Grant Nos. 11320101004, 11475243, and 11421505, the "100-talent plan" of Shanghai Institute of Applied Physics under Grant Nos. Y290061011 and Y526011011 from the Chinese Academy of Sciences, the "Shanghai Pujiang Program" under Grant No. 13PJ1410600, the US National Science Foundation under Grant No. PHY-1068022, the U.S. Department of Energy Office of Science under Award Number de-sc0013702, and the CUSTIPEN (China-U.S. Theory Institute for Physics with Exotic Nuclei) under the US Department of Energy Grant No. DE-FG02-13ER42025.

-
- [1] P. Danielewicz, R. Lacey, and W.G. Lynch, *Science* **298**, 1592 (2002).
 - [2] V. Baran, M. Colonna, V. Greco, and M. Di Toro, *Phys. Rep.* **410**, 335 (2005).
 - [3] B.A. Li, L.W. Chen, and C.M. Ko, *Phys. Rep.* **464**, 113 (2008).
 - [4] H. Liang, J. Meng, and S.G. Zhou, *Phys. Rep.* **570**, 1 (2015).
 - [5] J.E. Hirsch, *Phys. Rev. Lett.* **83**, 1834 (1999).
 - [6] M.I. Dyakonov and V.I. Perel, *Sov. Phys. JETP Lett.* **13**, 467 (1971).
 - [7] M.I. Dyakonov and V.I. Perel, *Phys. Lett. A* **459**, 35 (1971).
 - [8] Lecture notes of R. Machleidt, CNS summer school, University of Tokyo, Aug. 18-23, 2005.
 - [9] M.G. Mayer, *Phys. Rev.* **74**, 235 (1948); *Phys. Rev.* **75**, 1969 (1949).
 - [10] O. Haxel, J. Hans D. Jensen, and Hans E. Suess, *Phys. Rev.* **75**, 1766 (1949).
 - [11] D. Vautherin and D.M. Brink, *Phys. Rev. C* **5**, 626 (1972).
 - [12] P. Ring, *Prog. Part. Nucl. Phys.* **37**, 193 (1996).
 - [13] M. Bender, P. Heenen, and P.-G Reinhard, **75**, 121 (2003).
 - [14] P.-G. Reinhard, *Rep. Prog. Phys.* **52**, 439 (1989).
 - [15] A. Sulaksono *et al.*, *Ann. Phys.* **308**, 354 (2008).
 - [16] J.M. Pearson and M. Farine, *Phys. Rev. C* **50**, 185 (1994).
 - [17] B. G. Todd-Rutel *et al.*, *Phys. Rev. C* **69**, 021301(R) (2004).
 - [18] M. Grasso *et al.*, *Phys. Rev. C* **79**, 034318 (2009).
 - [19] O. Sorlin and M. G. Porquet, *Phys. Scr.* **T152**, 014003 (2013).
 - [20] P.-G. Reinhard and H. Flocard, *Nucl. Phys. A* **584**, 467 (1995).
 - [21] M.M. Sharma *et al.*, *Phys. Rev. Lett.* **74**, 3744 (1995).
 - [22] M. Onsi *et al.*, *Phys. Rev. C* **55**, 3166 (1997).
 - [23] J.M. Pearson, *Phys. Lett. B* **513**, 319 (2001).
 - [24] G.A. Lalazissis, D. Vretenar, W. Pöschl, and P. Ring, *Phys. Lett. B* **418**, 7 (1998).
 - [25] B.S. Pudliner *et al.*, *Phys. Rev. Lett.* **76**, 2416 (1996).
 - [26] J.P. Schiffer *et al.*, *Phys. Rev. Lett.* **96**, 162501 (2004) [Erratum-*ibid.*, **110**, 169901 (2013)]
 - [27] T. Lesinski *et al.*, *Phys. Rev. C* **76**, 014312 (2007).

- [28] M. Zalewski *et al.*, Phys. Rev. C **77**, 024316 (2008).
- [29] M. Bender *et al.*, Phys. Rev. C **80**, 064302 (2009).
- [30] Y.M. Engel *et al.*, Nucl. Phys. A **249**, 215 (1975).
- [31] T.H.R. Skyrme, Nucl. Phys. **9**, 615 (1958).
- [32] T. Otsuka, T. Suzuki, R. Fujimoto, H. Grawe, and Y. Akaishi, Phys. Rev. Lett. **95**, 232502 (2005).
- [33] T. Otsuka, T. Matsuo, and D. Abe, Phys. Rev. Lett. **97**, 162501 (2006).
- [34] T. Otsuka, T. Suzuki, M. Honma, Y. Utsuno, N. Tsunoda, K. Tsukiyama, and M. Hjorth-Jensen, Phys. Rev. Lett. **104**, 012501 (2010).
- [35] L. Gaudefroy *et al.*, Phys. Rev. Lett. **97**, 092501 (2006).
- [36] G. Colò, H. Sagawa, S. Fracasso, and P.F. Bortignon, Phys. Lett. B **646**, 227 (2007) [Erratum-ibid, **668**, 457 (2008)].
- [37] L.G. Cao, G. Colò, H. Sagawa, P.F. Bortignon, and L. Sciacchitano, Phys. Rev. C **80**, 064304 (2009).
- [38] C.L. Bai, H.Q. Zhang, H. Sagawa, X.Z. Zhang, G. Coló, and F.R. Xu, Phys. Rev. Lett. **105**, 072501 (2010).
- [39] C.L. Bai, H.Q. Zhang, H. Sagawa, X.Z. Zhang, G. Coló, and F.R. Xu, Phys. Rev. C **83**, 054316 (2011).
- [40] E.B. Suckling and P.D. Stevenson, Eur. Phys. Lett. **90**, 12001 (2010).
- [41] H.A. Bethe, Ann. Rev. Nucl. Part. Sci., **21**, 93 (1971).
- [42] V.R. Pandharipande, Nucl. Phys. A **181**, 33 (1972).
- [43] S. Fantoni and V.R. Pandharipande, Nucl. Phys. A **427**, 473 (1984).
- [44] S.C. Pieper, R.B. Wiringa, and V.R. Pandharipande, Phys. Rev. C **46**, 1741 (1992).
- [45] C. Ciofi degli Atti and S. Simula, Phys. Rev. C **53**, 1689 (1996).
- [46] A. Tang *et al.*, Phys. Rev. Lett. **90**, 042301 (2003).
- [47] K.S. Egiyan *et al.* (CLAS Collaboration), Phys. Rev. Lett. **96**, 082501 (2006).
- [48] E. Piassetzky, M. Sargsian, L. Frankfurt, M. Strikman, and J.W. Watson, Phys. Rev. Lett. **97**, 162504 (2006).
- [49] R. Subedi *et al.*, Science **320**, 1475 (2008).
- [50] O. Hen *et al.*, Science **346**, 614 (2014).
- [51] R. Schiavilla, R.B. Wiringa, S. C. Pieper, and J. Carlson, Phys. Rev. Lett. **98**, 132501 (2007).
- [52] M. Alvioli and C. Ciofi degli Atti, Phys. Rev. Lett. **100**, 162503 (2008).
- [53] J. Arrington, D.W. Higinbotham, G. Rosner, M. Sargsian, Prog. Part. Nucl. Phys. **67**, 898 (2012).
- [54] I. Vidaña, A. Polls, and C. Providencia, Phys. Rev. C **84**, 062801(R) (2011).
- [55] A. Carbone, A. Polls, and A. Rios, Eur. Phys. Lett. **97**, 22001 (2012).
- [56] C. Xu, A. Li, and B.A. Li, J. Phys.: Conf. Ser. **420**, 012190 (2013).
- [57] K. Pomorski and J. Dudek, Phys. Rev. C **67**, 044316 (2003).
- [58] O. Hen, B.A. Li, W.J. Guo, L.B. Weinstein, and E. Piassetzky, Phys. Rev. C **91**, 025803 (2015).
- [59] B.A. Li, W.J. Guo, and Z.Z. Shi, Phys. Rev. C **91**, 044601 (2015).
- [60] P. Hoodbhoy and J.W. Negele, Nucl. Phys. A **288**, 23 (1977).
- [61] K.T.R. Davies and S.E. Koonin, Phys. Rev. C **23**, 2042 (1981) [Erratum-ibid, **24**, 1820 (1981)].
- [62] A.S. Umar, M.R. Strayer, and P.-G. Reinhard, Phys. Rev. Lett. **56**, 2793 (1986).
- [63] P.-G. Reinhard *et al.*, Phys. Rev. C **37**, 1026 (1988).
- [64] A.S. Umar *et al.*, Phys. Rev. C **40**, 706 (1989).
- [65] J.A. Maruhn *et al.*, Phys. Rev. C **74**, 027601 (2006).
- [66] A.S. Umar and V.E. Oberacker, Phys. Rev. C **73**, 054607 (2006).
- [67] G.F. Dai, L. Guo, E.G. Zhao, and S.G. Zhou, Phys. Rev. C **90**, 044609 (2014).
- [68] Y. Iwata and J.A. Maruhn, Phys. Rev. C **84**, 014616 (2011).
- [69] G.F. Dai, L. Guo, E.G. Zhao, and S.G. Zhou, Sci. China-Phys. Mech. Astron. **57**, 1618 (2014).
- [70] P.D. Stevenson, E.B. Suckling, S. Fracasso, M.C. Barton, and A.S. Umar, arXiv: 1507.00645 [nucl-th].
- [71] C.Y. Wong, Phys. Rev. C **25**, 1460 (1982).
- [72] G.F. Bertsch and S. Das Gupta, Phys. Rep. **160**, 189 (1988).
- [73] J. Xu and B.A. Li, Phys. Lett. B **724**, 346 (2013).
- [74] Y. Xia, J. Xu, B.A. Li, and W.Q. Shen, Phys. Rev. C **89**, 064606 (2014).
- [75] Y. Xia, J. Xu, B.A. Li, and W.Q. Shen, arXiv: 1411.3057 [nucl-th].
- [76] J. Xu, B.A. Li, Y. Xia, and W.Q. Shen, Nucl. Phys. Rev. **31**, 306 (2014).
- [77] J. Xu, Y. Xia, B.A. Li, and W.Q. Shen, Nuclear Techniques **37**, 100513 (2014).
- [78] G.G. Ohlsen, Rep. Prog. Phys. **35**, 717 (1972).
- [79] W.G. Love and M.A. Franey, Phys. Rev. C **24**, 1073 (1981); **27**, 438 (1983).
- [80] P. Danielewicz and G. Odyniec, Phys. Lett. B **157**, 146 (1985).
- [81] V. Greco, C.M. Ko, and P. Lévai, Phys. Rev. Lett. **90**, 202302 (2003).
- [82] V. Greco, C.M. Ko, and P. Lévai, Phys. Rev. C **68**, 034904 (2003).
- [83] L.W. Chen, C.M. Ko, and B.A. Li, Nucl. Phys. A **729**, 809 (2003).
- [84] L.W. Chen, C.M. Ko, and B.A. Li, Phys. Rev. C **68**, 017601 (2003).
- [85] Y. Xia, J. Xu, B.A. Li, and W.Q. Shen, in preparation.
- [86] L.W. Chen, C.M. Ko, B.A. Li, and J. Xu, Phys. Rev. C **82**, 024321 (2010).
- [87] C. Hartnack *et al.*, Nucl. Phys. A **495**, 303 (1989).
- [88] J. Aichelin, Phys. Rep. **202**, 233 (1991).
- [89] C.C. Guo, Y.J. Wang, Q.F. Li, and F.S. Zhang, Phys. Rev. C **90**, 034606 (2014).
- [90] K. Asahi *et al.*, Phys. Lett. B **251**, 488 (1990).
- [91] H. Okuno *et al.*, Phys. Lett. B **335**, 29 (1994).
- [92] W.-D. Schmidt-Ott *et al.*, Z. Phys. A **350**, 215 (1994).
- [93] D.E. Groh *et al.*, Phys. Rev. Lett. **90**, 202502 (2003).
- [94] K. Asahi *et al.*, Phys. Rev. C **43**, 456 (1991).
- [95] D. Borremans *et al.*, Phys. Rev. C **66**, 054601 (2002).
- [96] K. Turzó *et al.*, Phys. Rev. C **73**, 044313 (2006).
- [97] Y. Ichikawa *et al.*, Nature Physics **8**, 918 (2012).
- [98] N.H. Buttigieg, E. Gotsman, and E. Leader, Phys. Rev. D **18**, 694 (1978).
- [99] A. Zelenski, G. Atoian, A. Bogdanov, D. Raparia, M. Runtso, and E. Stephenson, J. Phys.: Conf. Ser. **295**, 012132 (2011).